Report no. changed (Mar 2006): SM-371-UU

SACLANTCEN MEMORANDUM
serial no: SM- 371

SACLANT UNDERSEA RESEARCH CENTRE REPORT

Mode of PE predictions of propagation in range-dependent environments: SWAM'99 workshop results

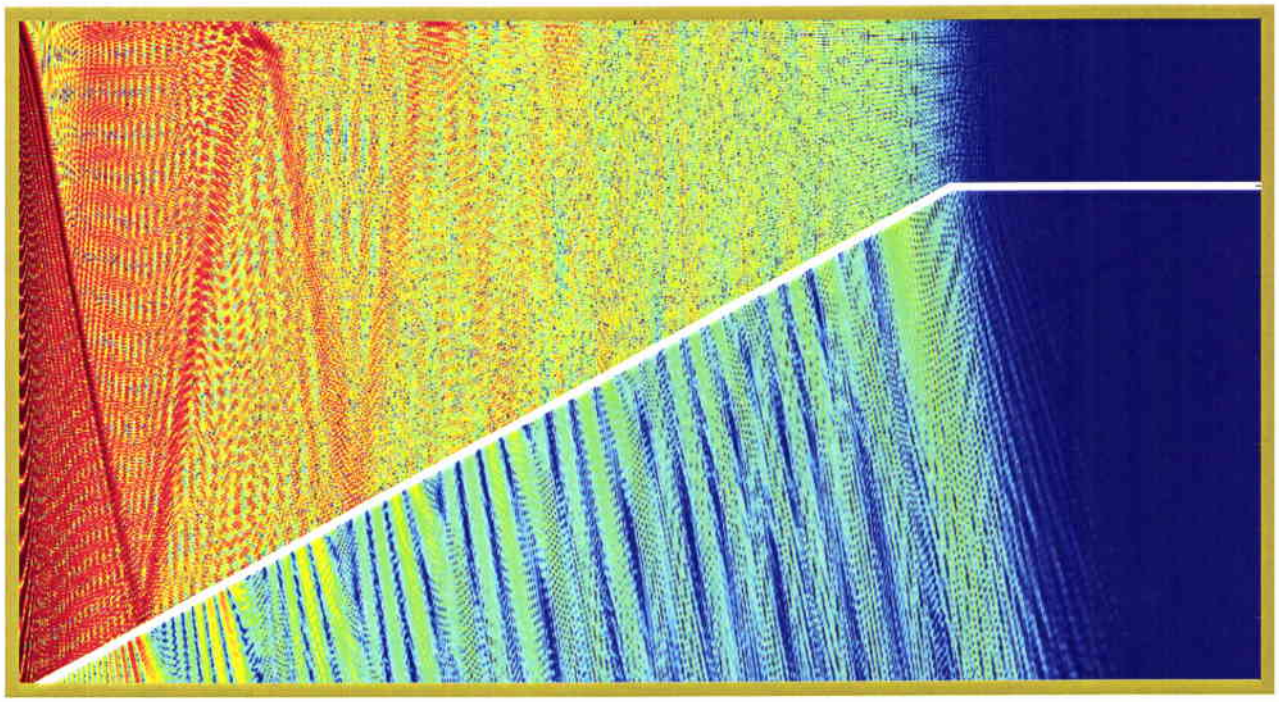

Peter L. Nielsen and Finn B. Jensen

May 2000

NORTH ATLANTIC TREATY ORGANIZATION ORGANISATION DU TRAITE DE L'ATLANTIQUE NORD

Mode and PE predictions of propagation in range-dependent environments: SWAM'99 workshop results.

P. L. Nielsen and F. B. Jensen

The content of this document pertains to work performed under Project 04-D of the SACLANTCEN Programme of Work. The document has been approved for release by The Director, SACLANTCEN.

Jan L. Spoelstra
Director

intentionally blank page

Mode and PE predictions of propagation in range-dependent environments: SWAM'99 workshop results.

P. L. Nielsen and F. B. Jensen

Executive Summary:

Prediction of sound propagation in complex range-dependent shallow water environments requires the application of numerical models. A variety of models exist with different levels of approximations in solving the propagation problem. If a high degree of accuracy is required, it is necessary to use sophisticated benchmark models. However, these models are too computationally intensive for practical applications and the solutions are often only used to validate newly developed "practical" models. Furthermore, the environmental information is usually sparse and although a highly accurate propagation model is applied in these cases, the solution may not represent the "true" propagation situation. The choice of propagation model for a specific underwater environment is therefore a compromise between required accuracy, computation time, amount of environmental information and post-processing requirements.

This report describes numerical propagation results of test cases defined for the SWAM'99 workshop, held at the Naval Postgraduate School, Monterey, CA, in Sept. 1999. The test cases consist of synthetic environments with range- and depth-dependent sound-speed profiles and bathymetry. Three practical propagation models with different levels of accuracy were applied to these range-dependent test cases. Environmental parameters used to generate runstreams for the acoustic models were known and the difference in the solutions is presented for these particular environments. In general, the results show consistency in received mean energy levels, but some differences in the coherent part of the acoustic field.

intentionally blank page

Mode and PE predictions of propagation in range-dependent environments: SWAM'99 workshop results.

P. L. Nielsen and F. B. Jensen

Abstract:

Three numerical acoustic models, a coupled normal-mode model (C-SNAP), an adiabatic normal-mode model (PROSIM) and a parabolic equation model (RAM), are applied to test cases defined for the SWAM'99 (**S**hallow-**W**ater **A**coustic **M**odeling) workshop, Naval Postgraduate School, Monterey (CA), 1999. The test cases consist of three shallow-water (flat bottom) scenarios with range-dependent sound-speed profiles imitating internal wave fields and a shelf-break case, with range-dependent sound-speed profiles and bathymetry. The bottom properties in all cases are range independent and modelled as a homogeneous fluid halfspace. The results from the modelling are presented as transmission loss for selected acoustic frequencies and source-receiver geometries and as received time series. The results are compared in order to evaluate the effect of applying different propagation models to the same range-dependent underwater environment. It should be emphasized that the propagation analysis is *not* an attempt to *benchmark* the selected propagation models, but to demonstrate the performance of practical, range-dependent models based on different approximations, in particular underwater scenarios.

Keywords: Numerical modelling ∘ coupled modes ∘ adiabatic modes ∘ parabolic equation ∘ range dependence

Contents

1 Introduction

Modelling of sound propagation in range-dependent, shallow-water environments is performed to enhance prediction capabilities by including realistic, detailed environmental information. The complexity of the environment requires a numerical solution to the range-dependent propagation problem as no general analytical solution is available. A variety of range-dependent propagation models exists with different levels of accuracy in computing sound propagation. Highly accurate models require prohibitively long execution time, which makes them unsuitable for practical applications. The solutions from these models are often only used to validate and assess the performance of newly developed models. Furthermore, the environmental input to the propagation models is often sparse and in these cases, a highly accurate propagation model does not necessarily describe the "true" propagation situation.

The choice of propagation model for a specific situation is therefore a compromise between accuracy, environmental information and computation time. In addition, the choice depends on the post-processing of output from the propagation model: Is the purpose of the modelling to compute mean received energy levels or complete time series ?

The **S**hallow-**W**ater **A**coustic **M**odeling (SWAM'99) workshop, held at the Naval Postgraduate School, Monterey, CA, September 15-17, 1999, was organized for the acoustics community to present state-of-the-art numerical modelling capabilities in range-dependent shallow-water environments. Six test cases were defined including combinations of 2D range-varying bathymetry, sound-speed profile and bottom properties and 3D propagation problems [1]. The purpose was to compare results from different range-dependent propagation models executed by different participants. The modelling results were given as transmission loss (TL) at selected frequencies and source-receiver geometries and time series. The workshop was organized as a "blind test", as no reference solution to the problems was available prior to the workshop.

Two range-dependent test cases were chosen from the workshop: (1) Internal wave test cases (IWA, IWB and IWC) with three different realizations of range-dependent sound-speed profiles in the water column and a flat bottom and (2) Shelf-break case including both range-dependent sound-speed profiles in the water column and changing bathymetry. For all test cases, the density and attenuation in the water column

is 1.0 g/cm^3 and 0.0 dB/λ, respectively. The bottom is modelled as a homogeneous fluid halfspace with a sound speed of 1700 m/s, density 1.5 g/cm^3 and attenuation 0.1 dB/λ.

Three different propagation models were used. The wide-angle parabolic equation model RAM [2], the coupled normal-mode model C-SNAP [3] and the adiabatic normal-mode model PROSIM [4]. RAM and C-SNAP are well established propagation models, which have been applied with confidence to numerous range-dependent propagation scenarios. The main difference between the models is that RAM includes the continuous spectrum (steep propagating paths above the critical angle at the bottom) and handles attenuation in the bottom correctly. C-SNAP only propagates the acoustic field described by a sum of discrete modes (paths in the water column below the critical angle), and utilizes a perturbation theory for the attenuation in the bottom. One-way mode-coupling is included in C-SNAP which allows for energy transfer between modes in range-dependent environments.

PROSIM is a range-dependent version of the real-wavenumber ORCA model [5]. Similar to C-SNAP, this model includes only the discrete modes and applies perturbation theory for bottom attenuation. PROSIM is a layered normal-mode model, which is more efficient than the finite-difference algorithm in C-SNAP for a moderate number of layers. In range-dependent environments, PROSIM utilizes the adiabatic approximation, which neglects coupling of energy between modes. When modelling time series by Fourier synthesis, PROSIM is the most efficient model as it performs interpolation of wavenumbers and mode functions in frequency. The frequency band of interest is divided into sub-bands and wavenumbers and mode functions are determined accurately at the limits of these sub-bands. Between the discrete frequency sub-band limits, wavenumbers and mode functions are interpolated with confidence, which reduces the number of frequency-by-frequency calculations. The efficiency of the model increases as the number of frequency components increases in the frequency band of interest.

The RAM and C-SNAP models approximate range-dependent environments by a sequence of range-independent sectors. RAM marches the complex pressure across the vertical sector interfaces and C-SNAP performs a modal-decomposition of the complex pressure to compute the modal excitation coefficients in the adjacent sector. The range-dependent environment for PROSIM is also divided into range-independent sectors, where the wavenumbers and mode functions are determined accurately at each sector interface. The wavenumbers and mode functions are then assumed to vary linearly in range within each sector.

The range-dependent environments for the test cases are given analytically. A careful convergence analysis of the calculations is performed by a refinement of the environmental and computational grid size until a stable solution to the acoustic propagation problem has been achieved. For comparison purposes the acoustic field

is calculated at the same ranges and depths within each model.

The source depth in the considered test cases is SD=30 m and the TL is calculated at frequencies of F=25, 250, 500 and 1000 Hz. The receiver depth is RD=35 and 70 m for the TL calculations as a function of range and the TL in depth is computed at ranges of R=5 and 15 km. For the frequencies above 25 Hz, the TL has been range- and depth-averaged by applying a running average window of 300 m in range and 5 m in depth. The received time series are modelled using C-SNAP and PROSIM by Fourier synthesis in the frequency band from 100 to 600 Hz in 0.5 Hz increments. This results in a total time window of 2 s. The time series are calculated at 35 and 70 m depths and at ranges of 5, 15 and 20 km. The source signature has a Gaussian spectrum with a center frequency of 375 Hz and bandwidth of 80 Hz. Only a subset of frequencies and source-receiver combinations are shown in the following, but the conclusions from these cases are applicable to the remaining results.

A reference solution for the test cases was not generated although accurate propagation models, the expertise to run them and the necessary computation facilities to obtain the results within a reasonable time are available [6, 7]. The purpose was to perform an inter-model comparison of propagation models for practical applications. The comparison of the TL results is done by stacking the TL curves *versus* range and depth from the models. The normalized Bartlett correlator is applied to perform a direct comparison between the received time series from the models. This correlation is often used as the objective function in geo-acoustic inversion as a measure (normalized Bartlett power) of mismatch between modelled and experimental data. The established measure has a value of 0 if the two signals are uncorrelated and a value of 1 if the signals are identical.

Two measures based on the Bartlett correlator are defined as follows:

$$B_d(r,f) = \frac{\left|\sum_{i=1}^{N_d} p_i^* \cdot q_i\right|}{\sqrt{\sum_{i=1}^{N_d} |p_i^* \cdot p_i|}\sqrt{\sum_{i=1}^{N_d} |q_i^* \cdot q_i|}} \tag{1}$$

$$B_f(r,z) = \frac{\left|\sum_{i=1}^{N_f} p_i^* \cdot q_i\right|}{\sqrt{\sum_{i=1}^{N_f} |p_i^* \cdot p_i|}\sqrt{\sum_{i=1}^{N_f} |q_i^* \cdot q_i|}} \tag{2}$$

where N_d and N_f is the number of depth points and frequency components, respectively. The complex pressure vectors from the two models are given by p_i and q_i and (*) denotes complex conjugate. The correlator in Eq. (1) corresponds to the generalized beamformer [8] and Eq. (2) corresponds to a matched filter (normalized cross-correlation) of the signals from the two models. In the calculation of the correlation the frequency increment was increased to 25 Hz in the band from 25 to

1000 Hz and the field sampling points were increased to 400 m in range and 50 m in depth.

The environmental discretization for the test cases and the computational grid size for the models are given in Table 1.

Table 1 *Environmental and computational discretization parameters.*

	IWA	IWB	IWC	Shelf break
C-SNAP	$DR^{(1)}$=40 m DZ =2 m	DR=40 m DZ=2 m	DR=40 m DZ=2 m	DR=2.5 m DZ=4 m
CPU-time CW (1 kHz) BB	 110 s 6 h	 55 s 3 h	 110 s 6 h	 3408 s 132 h
PROSIM	DR=40 m DZ =2 m	DR=40 m DZ=2 m	DR=40 m DZ=2 m	DR=10 m DZ=4 m
CPU-time CW (1 kHz) BB	 90 s 0.75 h	 50 s 0.40 h	 90 s 0.75 h	 230 s 10 h
RAM	DR=40 m DZ =2 m $\Delta R^{(2)}=5\cdot\Delta Z$ m $\Delta Z=\lambda/(20-50)$ m $Z_b^{(3)}$=220 - 1000 m	DR=40 m DZ=2 m $\Delta R=5\cdot\Delta Z$ m $\Delta Z=\lambda/(20-50)$ m Z_b=220 - 1000 m	DR=40 m DZ=2 m $\Delta R=5\cdot\Delta Z$ m $\Delta Z=\lambda/(20-50)$ m Z_b=220 - 1000 m	DR=40 m DZ=4 m $\Delta R=5\cdot\Delta Z$ m $\Delta Z=\lambda/(20-50)$ m Z_b=220 - 1000 m
CPU-time CW (1 kHz)	 596 s	 656 s	 655 s	 1541 s

(1) D is the discretization of the environmental input.

(2) Δ is computational discretization.

(3) Z_b is the depth to the truncation of the bottom, where the attenuation is increased to 10 dB/λ to prevent reflection.

The depth discretization ΔZ and the maximum depth Z_b for RAM are given in an interval due to the frequency dependency of the parameters. The CPU-times for the continuous wave (CW) and broadband (BB) computations refer to a COMPAQ Professional Workstation XP1000.

2

Internal waves

The internal wave cases consist of synthetically generated sound-speed profiles varying in range and depth by perturbing a single common background profile defined as:

$$\bar{c}(z) = \begin{cases} 1515 + 0.016 \cdot z & \text{for } z < 26\,\text{m} \\ c_0 \cdot \{1 + a\,[exp(-b) + b - 1]\} & \text{for } z \geq 26\,\text{m} \end{cases} \tag{3}$$

Here z is the depth coordinate, $c_0 = 1490$ m/s, $a = 0.25$ and $b = (z - 200)/500$. Three cases represent different scenarios of depth-range varying sound-speed profiles. The perturbation of the background profile for these three cases is given by an analytical expression to a range of 20 km with a constant water depth of 200 m.

2.1 *Internal wave case IWA*

Internal wave case IWA is defined as a sinusoidal perturbation of the background profile. The perturbation δc_{sin} is given by:

$$\delta c_{sin}(z, r) = C \cdot \frac{z}{B} \cdot \exp\left(\frac{-z}{B}\right) \cdot \cos(Kr) \tag{4}$$

where B =25 m, $K = 2\pi/(1000\,\text{m})$ and r is the range in metres measured from the acoustic source. The constant C is determined by allowing a maximum perturbation of 7.5 m/s. The final sound speed in case IWA is given by $\bar{c}(z) + \delta c_{sin}(z, r)$ [Fig. 1(a)].

The effect of introducing the perturbation of the background profile on the TL is determined by modelling the sound propagation through the background profile (range-independent environment) and the sinusoidal perturbation of the background profile. The results are obtained by C-SNAP (Fig. 2). The sinusoidal perturbation has little effect on TL at 25 Hz, where the interference of the acoustic field in range

and depth is almost identical. At higher frequencies, the perturbation clearly affects the TL by shifting the interference compared to the background profile result. However, the mean TL level is similar for both cases at higher frequencies.

The TL for test case IWA obtained by using the three range-dependent propagation models is shown in Fig. 3. The 25 Hz TL results are in very good agreement as the range-dependent profile has little effect at this frequency (Fig. 2). At close range, the effect of the continuous spectrum in RAM is seen as a slightly more varying TL than for the mode models. The contribution from the continuous spectrum is negligible at ranges beyond a few km because of the high attenuation. There is consistency in the results from C-SNAP and RAM at higher frequencies, whereas PROSIM deviates from the other models due to the adiabatic approximation. Mode coupling is significant at higher frequencies and it is necessary to include coupling to obtain the correct interference of the acoustic field. However, the mean TL is similar in all three models and the deviation of the adiabatic solution is of the same magnitude as shown in Fig. 2. Therefore, the mean TL does not change significantly when using only the background profile or when applying the adiabatic- or the coupled-mode models to the full range-dependent set of sound-speed profiles.

The source signature used in computation of the time series is shown in Fig. 4. The received time series (Fig. 5) are computed at three ranges and two depths. There is a large time dispersion of the signal in the problem which increases to the maximum range of 20 km. Here the signal is dispersed over a 1.6 s time window caused by the relative low attenuation and high sound speed in the bottom. Apparently, there is also good agreement in the individual arrival structure, indicating that the geometry in the problem is treated similarly by both models. However, differences in amplitude are clearly seen for some of the arrivals as in the TL calculations for certain ranges and depths at higher frequencies (Fig. 3).

The results from the correlation are shown in Fig. 6. The sound-speed profiles have a strong frequency- and range-dependent effect on the Bartlett power, B_d, between the coupled and adiabatic results [Fig. 6(a)]. The two fields are almost uncorrelated at ranges greater than 1 km and for frequencies above 200 Hz. At lower frequencies, the correlation is reasonable between the two models, but appears to become more frequency dependent at longer ranges. The Bartlett power, B_f, shows little correlation between the two fields except at close range. The full frequency band from 25 to 1000 Hz has been used and a higher correlation is obtained by reducing the maximum frequency in the calculation of B_f. Clearly this shows errors in using the adiabatic acoustic field coherently, when significant mode coupling is present in the propagation. Hence C-SNAP provides more accurate results than PROSIM.

2.2 Internal wave case IWB

Internal wave case IWB is a soliton perturbation of the background profile. The sound-speed perturbation is calculated as:

$$\delta c_{sol}(z,r) = C \cdot \frac{z}{B} \cdot \exp\left(\frac{-z}{B}\right) \sum_{i=1}^{6} A_i \left[\operatorname{sech}\left(\frac{R_i - r}{D_i}\right)\right]^2 \tag{5}$$

$$D_i = \sqrt{\frac{34300}{A_i}}$$

$$A_i = 10 \cdot \exp\left[-0.3 \cdot (i-1)\right]$$

$$R_i = R_{i-1} - 500 \cdot (7 - i) \qquad \text{(i>1)}$$

where R_1=14000 m and the value C is determined for a maximum perturbation of 12.5 m/s. The range- and depth-dependent profile for case IWB is calculated as $\bar{c}(z) + \delta c_{sol}(z,r)$ [Fig. 1(b)]. Notice the 6 distinct soliton-like features appearing in the range between 5 and 15 km. The sound speed at a short range from the features is almost the same as the range-independent background profile.

The TL calculated by the three models for this case (Fig. 7) is very similar. Almost identical results are obtained for the first 5 km as the environment is range-independent. Differences in the results between PROSIM and C-SNAP/RAM can be observed as the field is propagated across the soliton-like features, particularly at higher frequencies. The features in the water column redistribute the acoustic energy causing the adiabatic model to give erroneous results. Notice the excellent agreement between C-SNAP and RAM at all ranges, depths and frequencies. The mean TL level is similar to case IWA.

The time series are in perfect agreement between C-SNAP and PROSIM at ranges before the first soliton-like feature. At longer ranges, when the field has propagated through the range-dependent part of the water column, the conclusions are the same as for case IWA.

The excellent agreement between the adiabatic- and coupled-mode solution is also seen in the Bartlett power (Fig. 8). The correlation B_d and B_f is one for all depths and frequencies before the range of the first soliton. The correlations decreases abruptly as the acoustic field propagates through each of the features in the sound speed. At ranges between the solitons, the correlation is almost constant in both frequency and depth as the environment is close to range-independent. The B_d has a high value at long ranges up to a frequency of around 400 Hz and at higher

frequencies the fields are close to uncorrelated [Fig. 8(a)]. This is also seen for B_f, where the correlation is low for long ranges and for all depths. The full frequency band is used in this calculation, which may cause the low correlation (B_f) at long ranges. In general, the correlation is higher in this case compared to the IWA case.

2.3 Internal wave case IWC

The last internal wave case (IWC) is a combination of case IWB with an additional perturbation to the background profile as following:

$$\delta c_{sins}(z,r) = C \cdot \frac{z}{B} \cdot \exp\left(\frac{-z}{B}\right) \sum_{i=1}^{5} \cos(K_i r) \tag{6}$$

$$K_i = \frac{2\pi}{2000 - 300 \cdot (i-1)}$$

where B=25 m and C is determined to produce a maximum perturbation $\delta c_{sins}(z,r)$ of 7.5 m/s [Fig. 1(c)].

The TL from the three models (Fig. 9) is the same as case IWA (Fig. 3). There is very good agreement between C-SNAP and RAM for all ranges, depths and frequencies. The adiabatic solution deviates especially at higher frequencies, but the mean TL levels are fairly well determined. The received time series for this case are similar to cases IWA and IWB.

The correlation B_d [Fig. 10(a)] decreases smoothly as a function of range and frequency. The correlation is higher than in IWA and lower than in IWB reflecting the different levels of complexity in the sound-speed profiles. At long range, the correlation remains relatively high for frequencies below a few hundred Hz. The correlation B_f decreases rapidly within the first km of propagation, remaining low for all ranges and depths, as seen in case IWA. Again, the maximum frequency of 1000 Hz included in the computation of B_f may be the reason for the fast decrease in the correlation.

3

Shelf break

In the shelf-break case the bathymetry and the sound-speed profiles are range dependent [Fig. 1(d)]. The water depth at 0 km range is 400 m and the depth decreases linearly to 100 m at a range of 15 km (1.15° up-slope). Hereafter the depth is constant 100 m to a range of 20 km. The sound-speed profile changes from a deep-water profile at the acoustic source to a shallow-water profile. The transition appears through a front-like feature at a range of 10 km.

The sound-speed profile $c(z,r)$ is defined as:

$$
\begin{aligned}
c(z,r) &= 1450 + 4.6 \cdot T(z,r) - 0.055 \cdot T^2(z,r) + 0.016 \cdot z \qquad (7)\\
T(z,r) &= 5 + T_0(r) \cdot \sinh\left[\frac{\pi(400-z)}{53000}\right]\\
T_0(r) &= 15 - 5\left[1 + \tanh\left(r \cdot 10^{-3} - 10\right)\right]
\end{aligned}
$$

where $T(r,z)$ is the range- and depth-dependent temperature and $T_0(r)$ is the range-dependent surface temperature in °C.

The RAM model deviates slightly from the normal-mode models in the TL levels at 25 Hz out to a range of around 14.5 km (Fig. 11). The reason for this difference is that the continuous spectrum contributes to the propagating field at this frequency. This has been verified by defining a high-speed false bottom in the C-SNAP model which discretizes the continuous spectrum. In this case the two results agree, but the false bottom causes a significant increase in computation time as the number of modes increases. This effect is less important at higher frequencies where there is excellent agreement between the models out to 14.5 km.

At around 15 km in range, there is an abrupt change in TL which becomes more pronounced at higher frequencies. At 1000 Hz the TL increases from 70 to 95 dB within a few hundred metres, but RAM propagates higher field levels out to longer ranges than the normal-mode models. The reason for this is that RAM includes the contribution from the steep-angle continuous spectrum, which results in a 15 dB

difference in TL between the RAM and the mode models for all depths. At ranges greater than 16 km the models appear to converge towards the same solution.

The abrupt increase in TL at around 14.5 km is due to a combination of sound-speed profile, acoustic frequency, bottom sound speed and bottom slope. This is illustrated by the TL calculations at 1000 Hz using RAM in Fig. 12. The results are obtained with low attenuation in the bottom (0.05 dB/λ) and by using only the shallow-water (the sound-speed profile at 20 km range) and the deep-water profile (the sound-speed profile at 0 km range). In the case of the shallow-water profile, the acoustic field propagates at a relatively shallow angle, which becomes steeper as the field propagates up-slope. A part of the field exceeds the critical angle and is lost into the bottom. However, the main part of the field stays in the water column out to the shallow-water region at ranges beyond 15 km.

The acoustic field for the deep-water profile propagates initially at steeper angles than for the shallow-water profile (the source is located in the high-speed thermocline). As the field propagates up-slope, the main part of the field exceeds the critical angle and is lost into the bottom, at a range of around 14.5 km. Little energy is transmitted into the shallow-water region. The high loss of energy is strongly dependent on the sound-speed profile, but the range-dependence of the sound speed in the original problem has only a minor impact on propagation conditions. The solution to this problem is very sensitive to the excitation of the field at the source location and the inclusion of the continuous spectrum. RAM solves the full-field problem and is here considered to give the correct solution.

The time series computed by C-SNAP and PROSIM are in agreement to the same degree as seen in case IWA. The correlation of the complex acoustic fields from the two models is shown in Fig. 13. The correlation B_d increases with frequency as the acoustic field propagates towards the shallow-water region. In general the correlation is low for frequencies above 400 Hz at long ranges. An abrupt decrease in B_d is seen at close range and at a frequency above 200 Hz for this problem. The value of B_f is high at all ranges for depths down to 150 m. The correlation is low at greater depths, which may be due to a poor representation of the wavenumbers and mode functions in PROSIM at these depths.

4

Conclusions

A subset of range-dependent test cases defined for the SWAM'99 workshop has been chosen for comparing results from three range-dependent propagation models. The mean transmission loss for the internal wave cases are in good agreement between the parabolic equation, coupled-mode and the adiabatic propagation models. The range-independent background sound-speed profile was sufficient to compute the mean TL levels obtained by including the full range-dependent profiles. The interference properties of the transmission loss are clearly affected by the presence of the range-dependent sound-speed structure. The parabolic equation and the coupled-mode solutions are in excellent agreement. The adiabatic model shows deviations in levels at certain depths and ranges.

There is consistency in the arrival structure of the received time series between the couple-mode and the adiabatic model. This indicates that the geometry in the problem is treated similarly in both models. However, amplitude differences appear as can be seen in the transmission loss modelling. The correlation between the coupled-mode and adiabatic model is range and frequency dependent. In general, the correlation is high at close range and low frequency decreasing abruptly at longer ranges and higher frequencies.

Similar conclusions are found for the shelf-break case, in which there is excellent agreement between the three models in the coherent transmission loss for up-slope propagation. Close to the shallow-water region, the importance of choosing the correct propagation model is demonstrated. Almost all energy trapped in the water column is lost into the bottom for the mode models. The parabolic equation model propagates higher levels out to longer ranges, because of the correct excitation of the field at the source, and the inclusion of the continuous spectrum. The abrupt loss of energy into the bottom is highly sensitive to the sound-speed profile in the water, bottom properties, slope of the bathymetry and the acoustic frequency. This test case is the most demanding of the test cases considered concerning the accuracy of the numerical model.

There is consistency in the results from the parabolic equation and the coupled-mode model. The adiabatic model clearly shows deviations in the cases of significant range dependence, when the adiabatic results are correlated with the coupled-mode results. The mean TL levels are in good agreement with the other two models

and the adiabatic model is superior in computation time for broadband, range-dependent propagation modelling. The difficulties in applying the adiabatic model are *not* general, as the success of propagation predictions using this type of model depends on the specific underwater environment. The adiabatic model is sufficiently accurate for pratical applications in the majority of range-dependent environments, as the lack of environmental information is often the limiting factor.

References

[1] Tolstoy, A. *et al*, Tentatively titled: Review of results for SWAM'99, submitted to *Journal of Computational Acoustics.*

[2] Collins, M.D. A split-step Padé solution for parabolic equation method. *Journal of the Acoustical Society of America*, **93**, 1993:1736-1742.

[3] Ferla, C.M., Jensen, F.B. C-SNAP: Coupled SACLANTCEN normal-mode propagation loss model, SACLANTCEN SM-274, 1993.

[4] Bini-Verona, F., Nielsen, P.L., Jensen, F.B. PROSIM broadband normal-mode model: A user's guide, SACLANTCEN SM-358, 2000.

[5] Westwood, E.K., Tindle, C.T., Chapman, N.R. A normal-mode model for acousto-elastic ocean environments, *Journal of the Acoustical Society of America* **100**, 1996:3631-3645.

[6] Jensen, F.B., Ferla, C.M. Numerical solutions of range-dependent benchmark problems in ocean acoustics, *Journal of the Acoustical Society of America* **87**, 1990:1499-1510.

[7] Jensen, F.B., Ferla, C.M., Gerstoft, P. Benchmarking scattering in ocean waveguides, SACLANTCEN SM-290, 1995.

[8] Jensen, F.B., Kuperman, W.A., Porter, M.B., Schmidt, H. *Computational Ocean Acoustics*, New York, AIP Press, 1994.

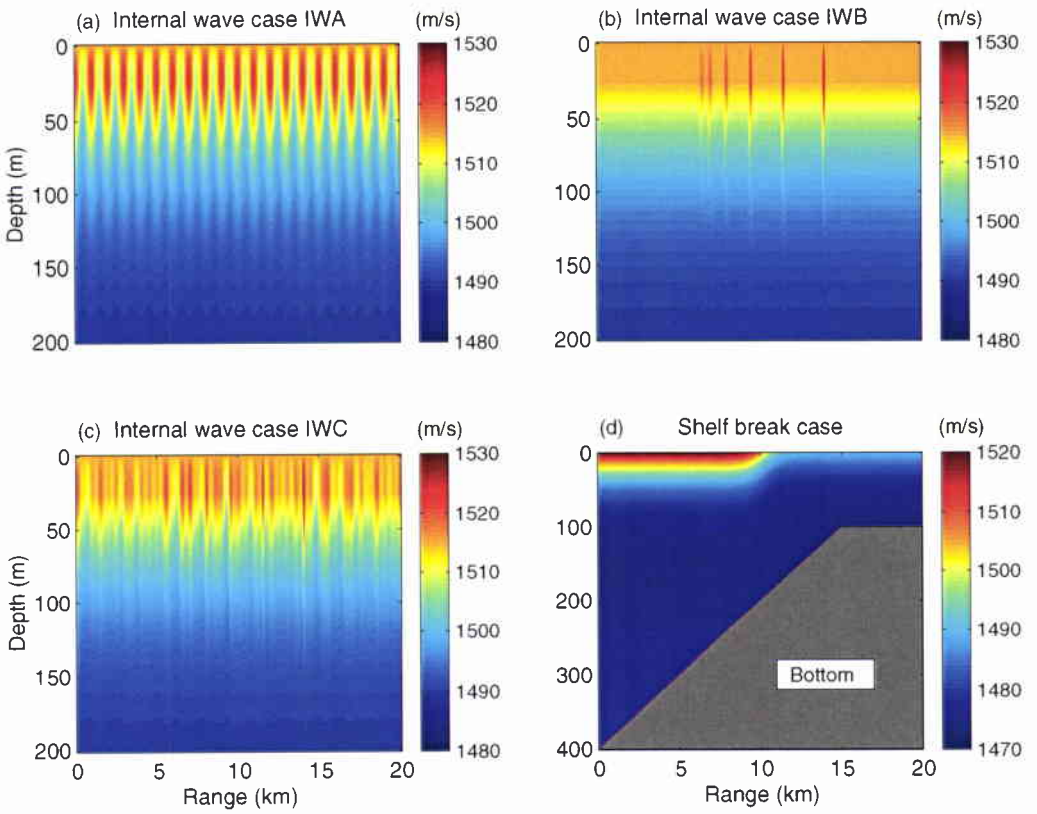

Figure 1 *Schematic of range- and depth-dependent environments for the internal wave cases and the shelf-break case.*

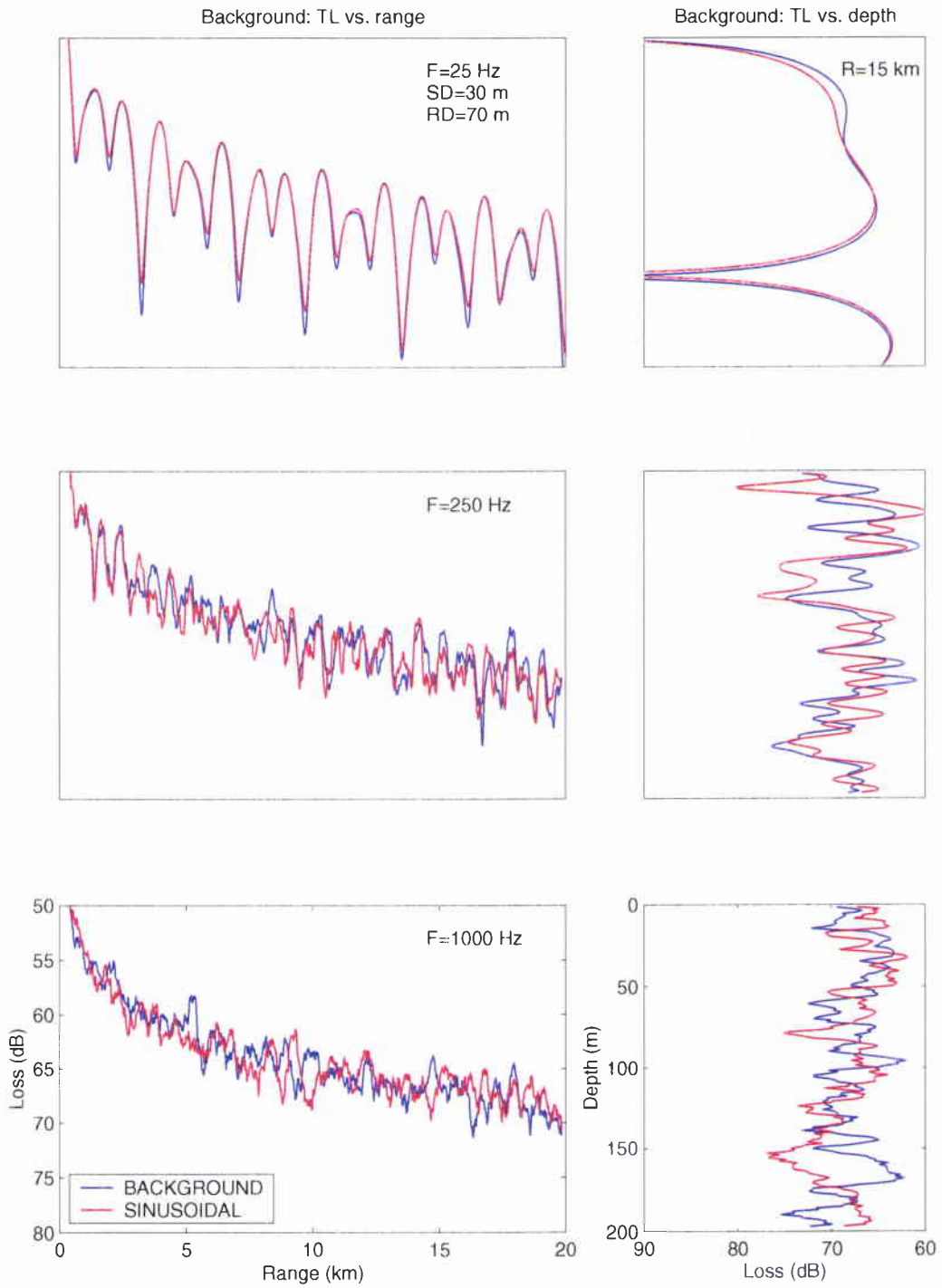

Figure 2 *Transmission loss as a function of range and depth for the background profile and the IWA case. The results are obtained by* C-SNAP *at frequencies of F=25, 250 and 1000 Hz.*

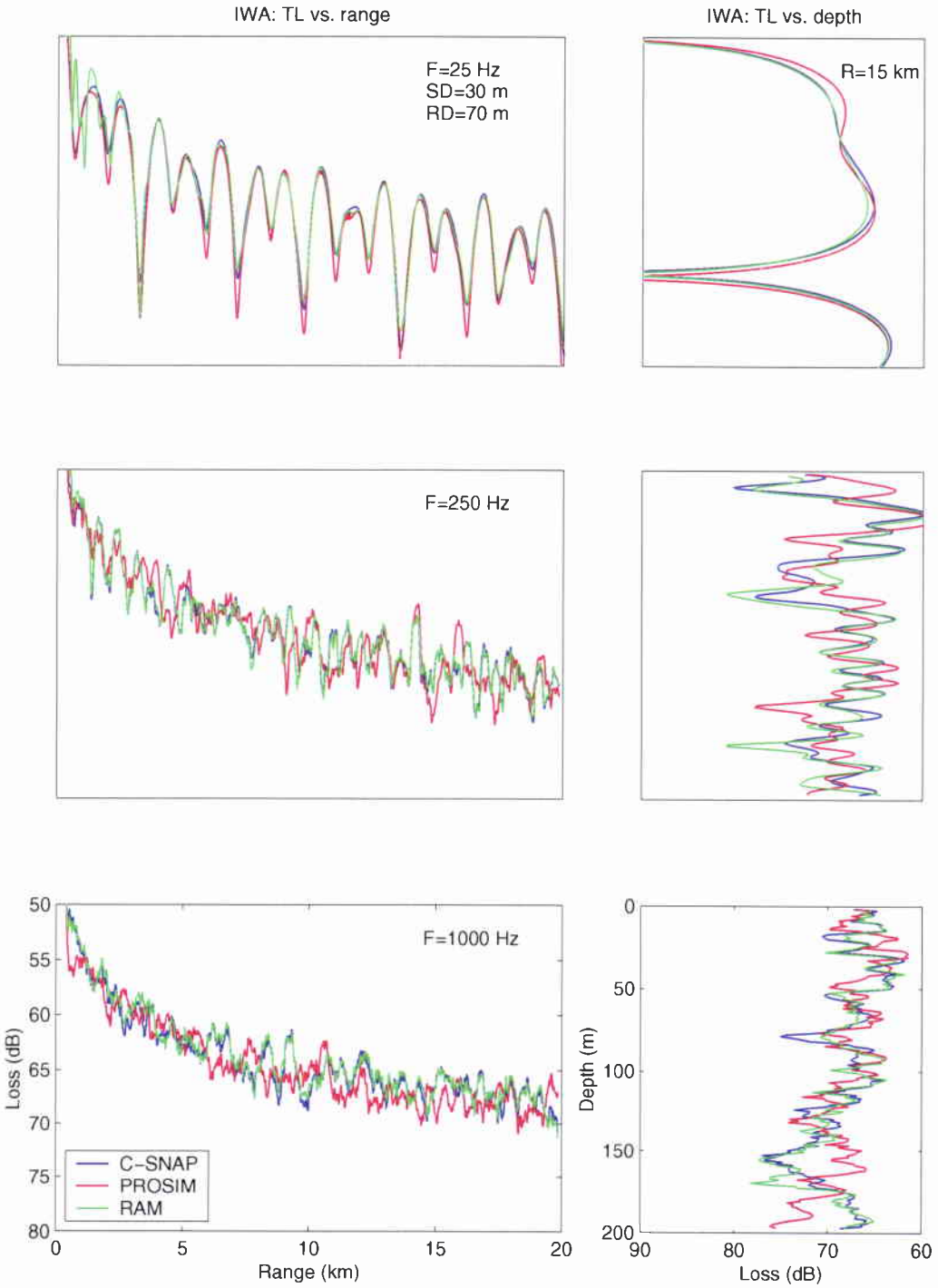

Figure 3 *Transmission loss as a function of range and depth for case IWA. The results are obtained by all three models* (C-SNAP, PROSIM, RAM) *at frequencies of F=25, 250 and 1000 Hz.*

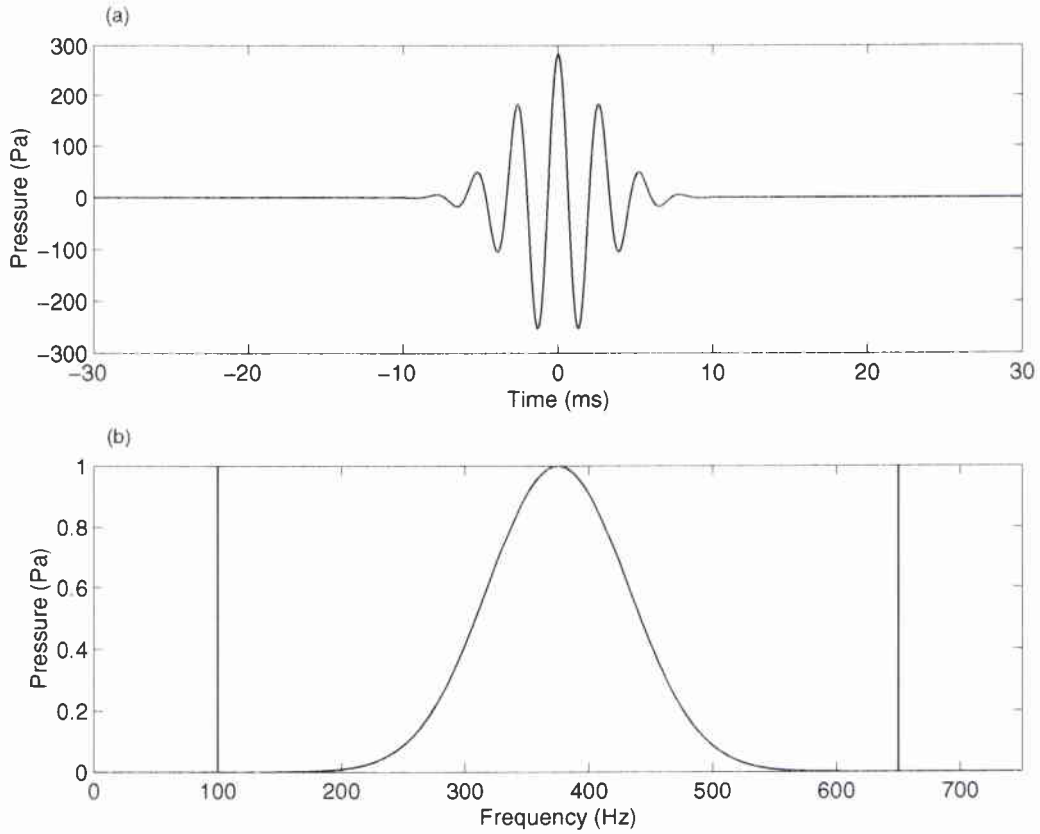

Figure 4 *Gaussian pulse (a) and spectrum (b) used in the modelling of broadband received time series.*

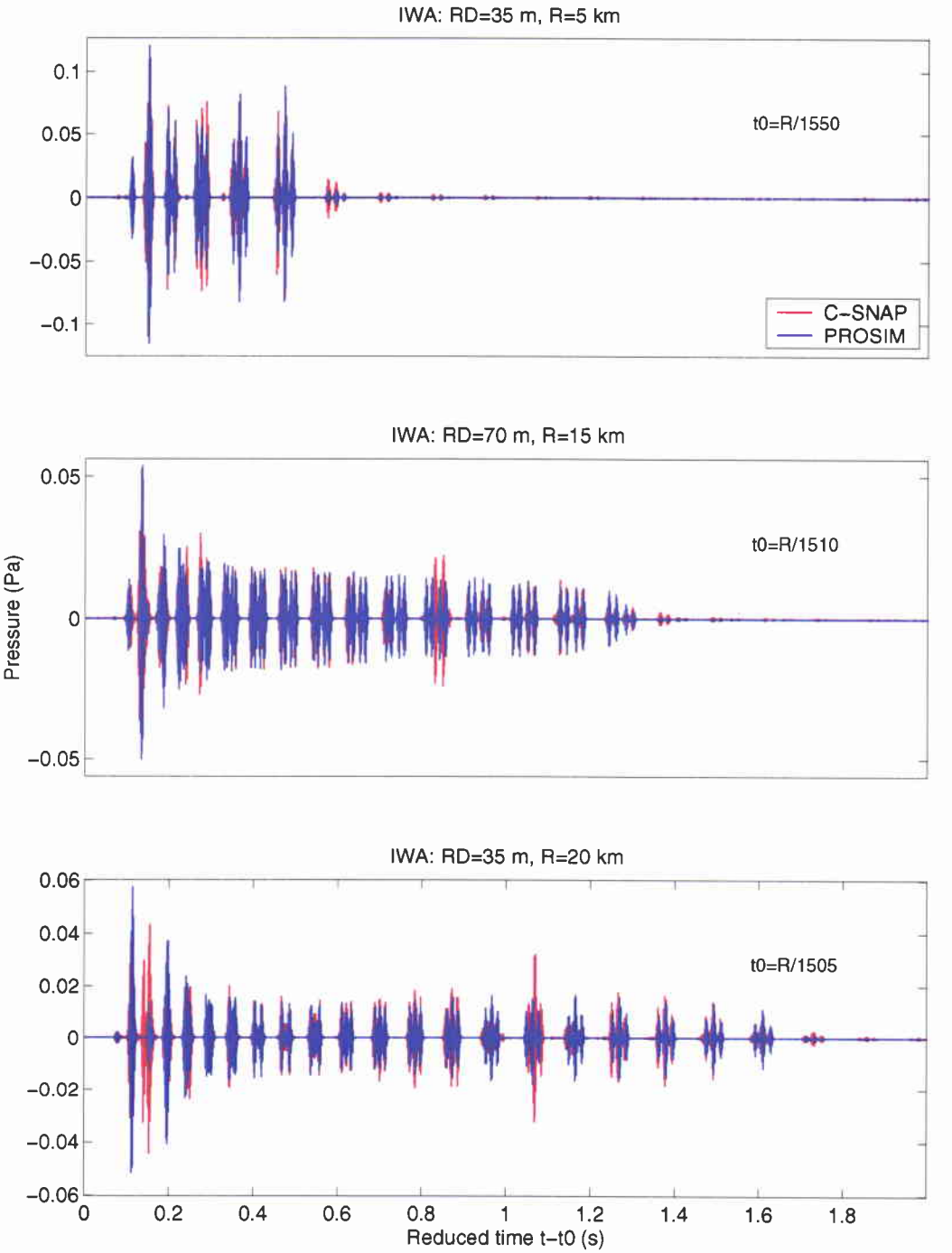

Figure 5 *Received time series computed by* C-SNAP *and* PROSIM *for case IWA.*

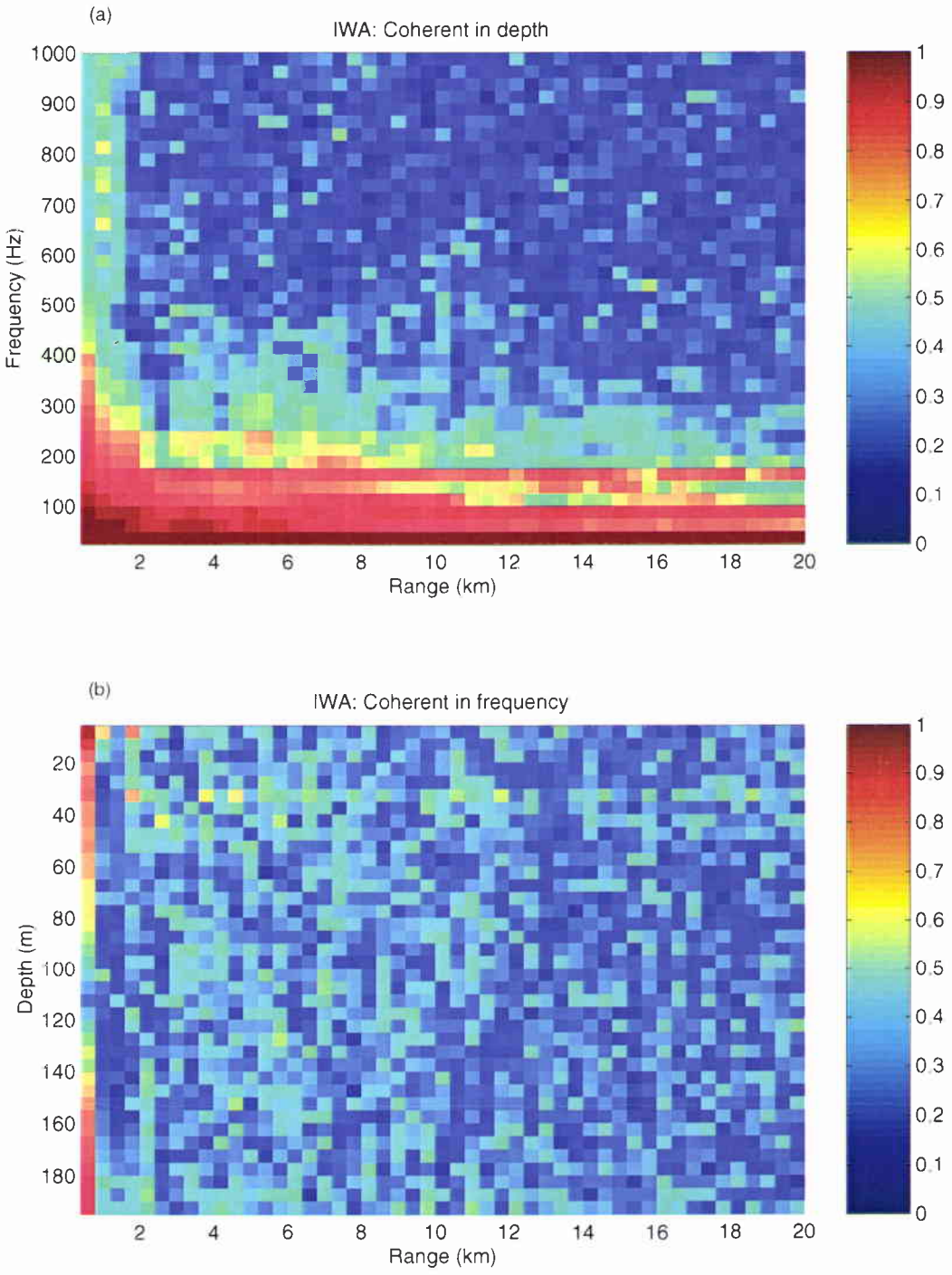

Figure 6 *Bartlett correlator applied to the results from* C-SNAP *and* PROSIM *for case IWA. (a) Normalized Bartlett power with the complex pressure added coherently in depth (B_d) and (b) the complex pressure added coherently in frequency (B_f).*

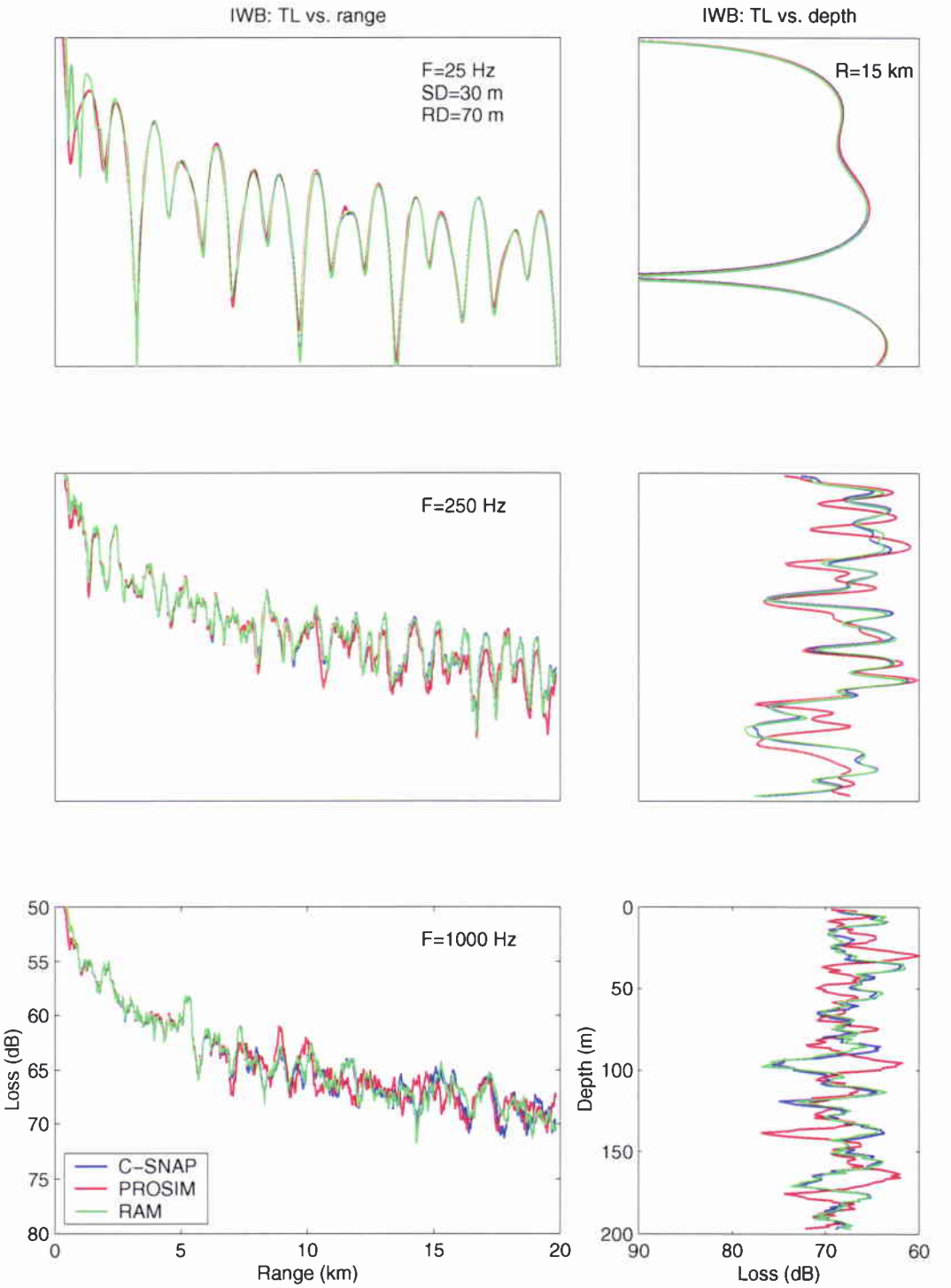

Figure 7 *Transmission loss as a function of range and depth for case IWB. The results are obtained by all three models* (C-SNAP, PROSIM, RAM) *at frequencies of F=25, 250 and 1000 Hz.*

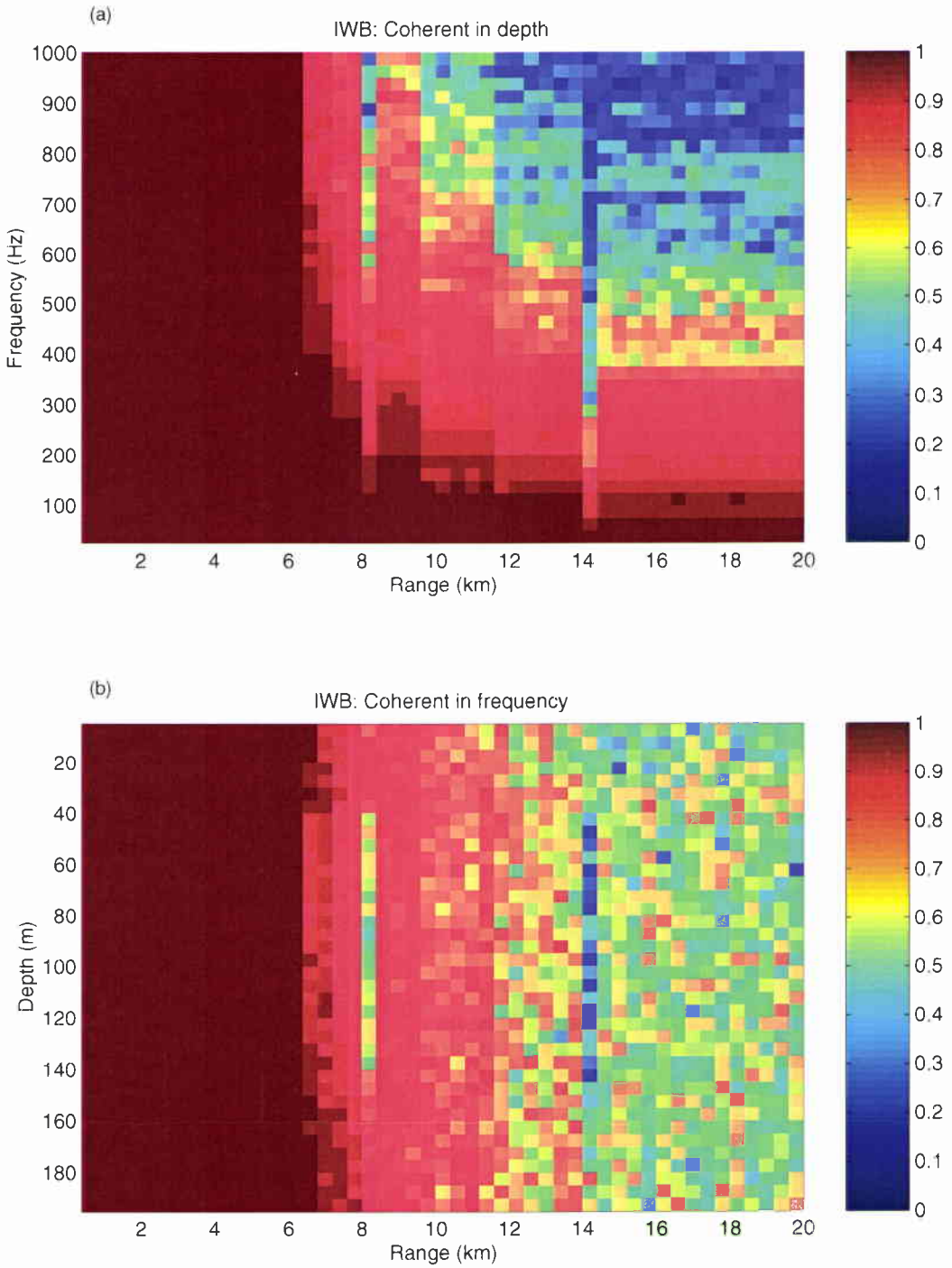

Figure 8 *Bartlett correlator applied to the results from* C-SNAP *and* PROSIM *for case IWB. (a) Normalized Bartlett power with the complex pressure added coherently in depth (B_d) and (b) the complex pressure added coherently in frequency (B_f).*

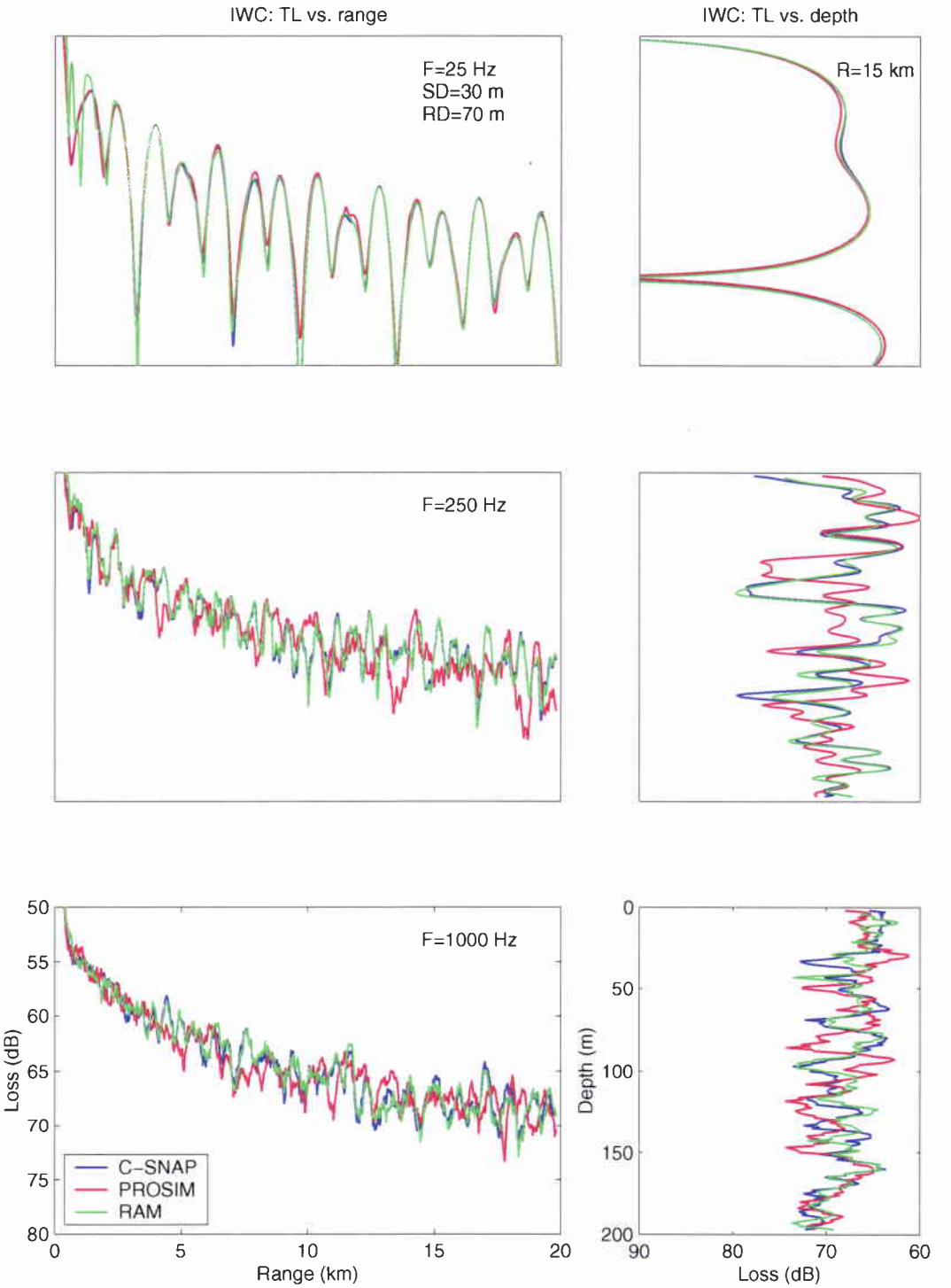

Figure 9 *Transmission loss as a function of range and depth for case IWC. The results are obtained by all three models* (C-SNAP, PROSIM, RAM) *at frequencies of F=25, 250 and 1000 Hz.*

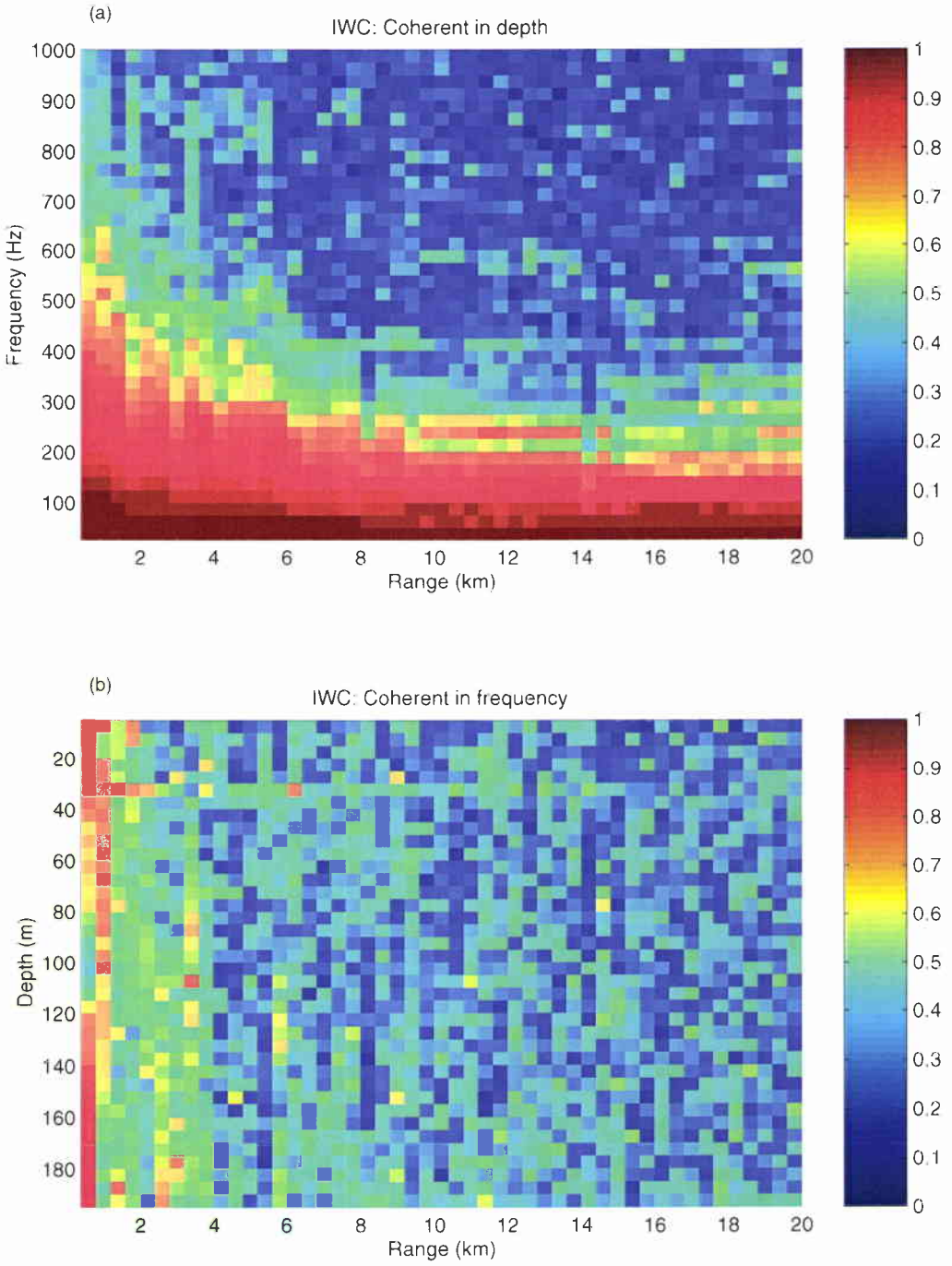

Figure 10 *Bartlett correlator applied to the results from* C-SNAP *and* PROSIM *for case IWC. (a) Normalized Bartlett power with the complex pressure added coherently in depth (B_d) and (b) the complex pressure added coherently in frequency (B_f).*

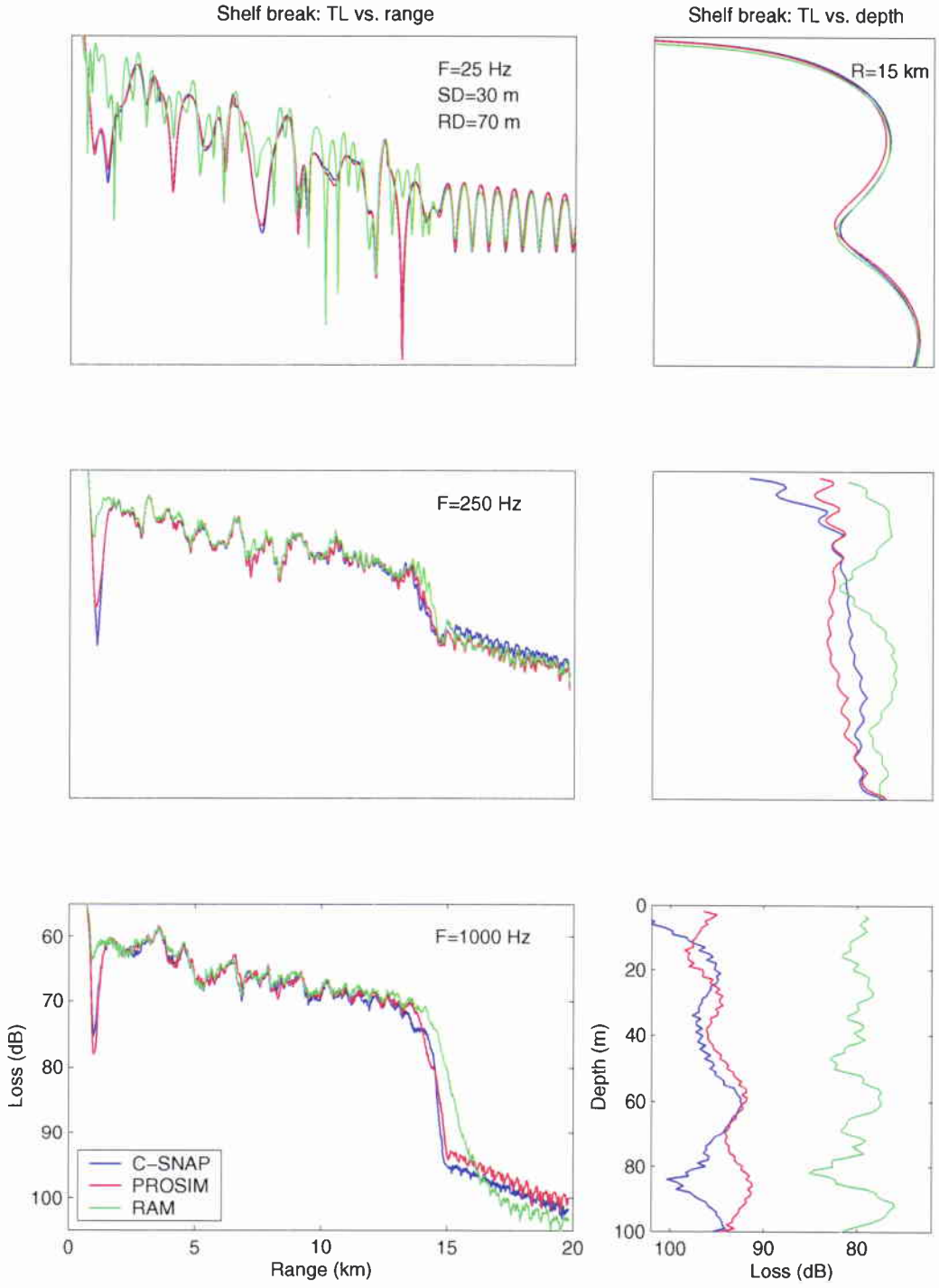

Figure 11 *Transmission loss as a function of range and depth for the shelf-break case. The results are obtained by all three models* (C-SNAP, PROSIM, RAM) *at frequencies of F=25, 250 and 1000 Hz.*

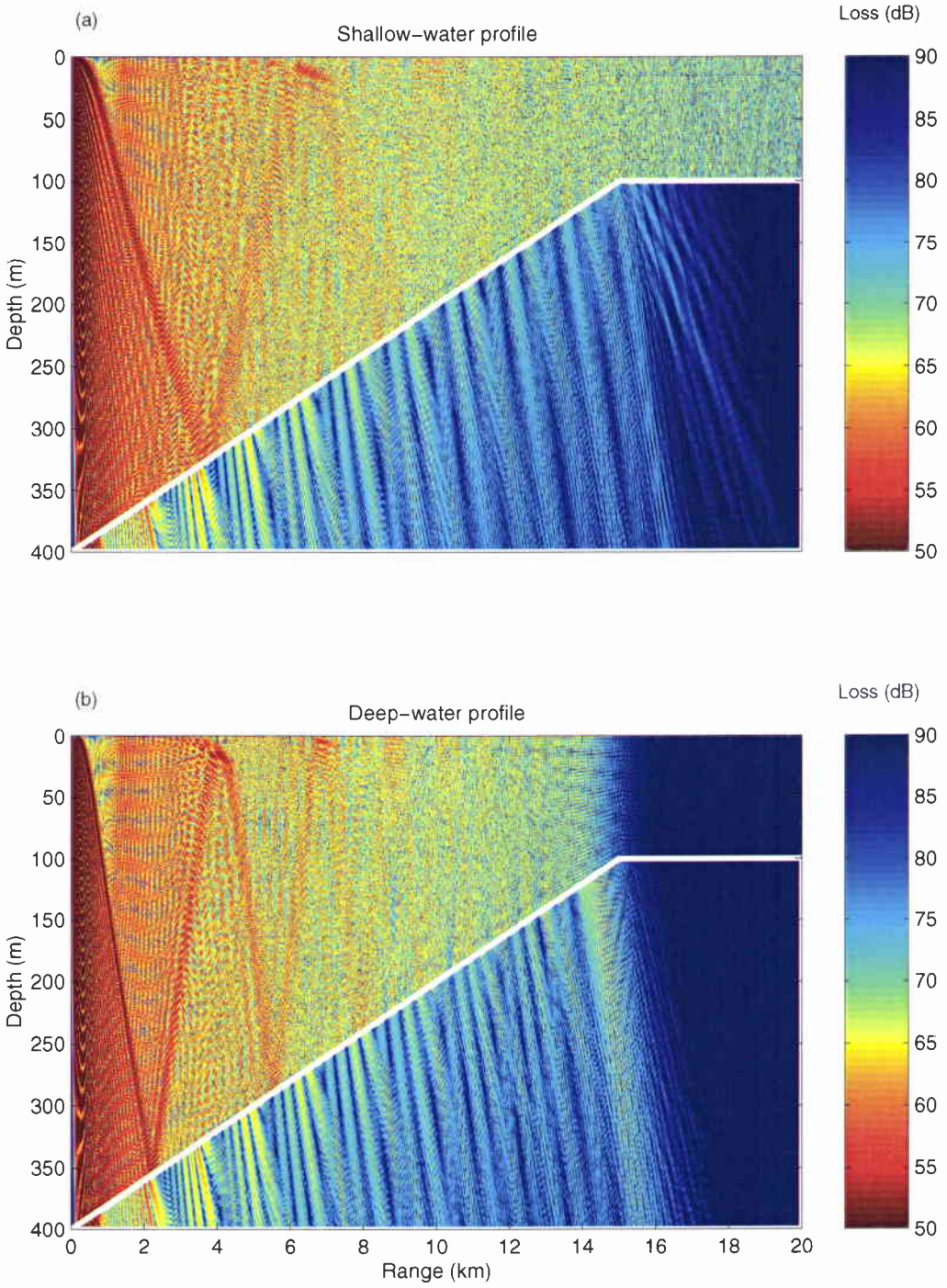

Figure 12 *Transmission loss as a function of depth and range using the shallow- and deep-water sound-speed profile. The results are obtained by* RAM *at a frequency of 1000 Hz.*

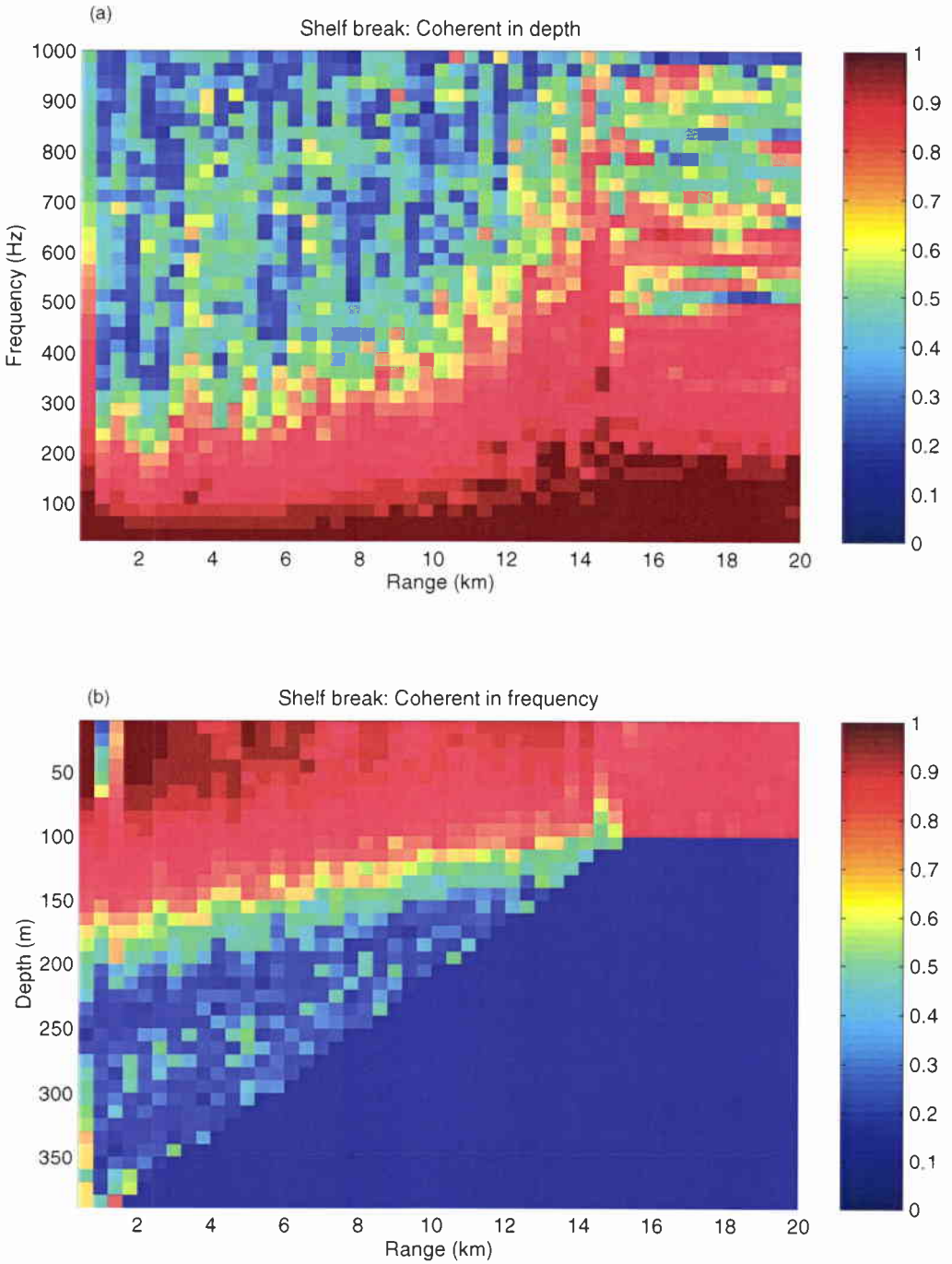

Figure 13 *Bartlett correlator applied to the results from* C-SNAP *and* PROSIM *for the shelf-break case. (a) Normalized Bartlett power with the complex pressure added coherently in depth (B_d) and (b) the complex pressure added coherently in frequency (B_f).*

Report no. changed (Mar 2006): SM-371-UU

Document Data Sheet

Security Classification		Project No.
UNCLASSIFIED		04-D
Document Serial No.	**Date of Issue**	**Total Pages**
SM-371	April 2000	31 pp.

Author(s)

Nielsen, P.L., Jensen, F.B.

Title

Mode and PE predictions of propagation in range-dependent environments: SWAM'99 workshop results.

Abstract

Three numerical acoustic models, a coupled normal-mode model (C-SNAP), an adiabatic normal-mode model (PROSIM) and a parabolic equation model (RAM), are applied to test cases defined for the SWAM'99 (Shallow- Water Acoustic Modeling) workshop, Naval Postgraduate School, Monterey (CA), 1999. The test cases consist of three shallow-water (flat bottom) scenarios with range-dependent sound-speed profiles imitating internal wave fields and a shelf-break case, with range-dependent sound-speed profiles and bathymetry. The bottom properties in all cases are range independent and modelled as a homogeneous fluid halfspace. The results from the modelling are presented as transmission loss for selected acoustic frequencies and source-receiver geometries and as received time series. The results are compared in order to evaluate the effect of applying different propagation models to the same range-dependent underwater environment. It should be emphasized that the propagation analysis is not an attempt to benchmark the selected propagation models, but to demonstrate the performance of practical, range-dependent models based on different approximations, in particular underwater scenarios.

Keywords

Numerical modelling - coupled modes - adiabatic modes - parabolic equation - range dependence

Issuing Organization

North Atlantic Treaty Organization
SACLANT Undersea Research Centre
Viale San Bartolomeo 400, 19138 La Spezia, Italy

[From N. America: SACLANTCEN (New York) APO AE 09613]

Tel: +39 0187 527 361
Fax:+39 0187 527 700

E-mail: library@saclantc.nato.int

The SACLANT Undersea Research Centre provides the Supreme Allied Commander Atlantic (SACLANT) with scientific and technical assistance under the terms of its NATO charter, which entered into force on 1 February 1963. Without prejudice to this main task - and under the policy direction of SACLANT - the Centre also renders scientific and technical assistance to the individual NATO nations.

SACLANT Undersea Research Centre
Viale San Bartolomeo 400
19138 San Bartolomeo (SP), Italy

tel: +39 0187 527 (1) or extension
fax: +39 0187 527 700

e-mail: library@saclantc.nato.int

NORTH ATLANTIC TREATY ORGANIZATION